Commun Nonlinear Sci Numer Simulat 45 (2017) 158–175

Contents lists available at ScienceDirect

Commun Nonlinear Sci Numer Simulat

journal homepage: www.elsevier.com/locate/cnsns

Research paper

Transient response of an active nonlinear sandwich piezolaminated plate

Atta Oveisi[a,*], Tamara Nestorović[b]

[a] Ruhr-Universität Bochum, Mechanics of Adaptive Systems, Institute of Computational Engineering, (ICFW 03-523), Universitätsstr. 150, D-44801 Bochum, Germany

[b] Ruhr-Universität Bochum, Mechanics of Adaptive Systems, (ICFW 03-725), Universitätsstr. 150, D-44801 Bochum, Germany

ARTICLE INFO

Article history:
Received 23 February 2016
Revised 15 August 2016
Accepted 17 September 2016
Available online 20 September 2016

Keywords:
Geometrical nonlinearity
Vibration control
Semi-analytical approach
Transient response

ABSTRACT

In this paper, the dynamic modelling and active vibration control of a piezolaminated plate with geometrical nonlinearities are investigated using a semi-analytical approach. For active vibration control purposes, the core orthotropic elastic layer is assumed to be perfectly bonded with two piezo-layers on its top and bottom surfaces which act as sensor and actuator, respectively. In the modelling procedure, the piezo-layers are assumed to be connected via a proportional derivative (PD) feedback control law. Hamilton's principle is employed to acquire the strong form of the dynamic equation in terms of additional higher order strain expressions by means of von Karman strain-displacement correlation. The obtained nonlinear partial differential equation (NPDE) is converted to a system of nonlinear ordinary differential equations (NODEs) by engaging Galerkin method and using the orthogonality of shape functions for the simply supported boundary conditions. Then, the resulting system of NODEs is solved numerically by employing the built-in Mathematica function, "NDSolve". Next, the vibration attenuation performance is evaluated and sensitivity of the closed-loop system is investigated for several control parameters and the external disturbance parameters. The proposed solution in open loop configuration is validated by finite element (FE) package ABAQUS both in the spatial domain and for the time-/frequency-dependent response.

1. Introduction

The unwanted vibrations with high amplitude due to excitations at or close to resonance frequencies of mechanical structures is one of the main reasons for mechanical malfunctions and failure. In order to be able to predict and possibly prevent such phenomena, model-based investigation of the structural behavior in early development phases plays an important role. One of the first steps in the modeling procedure is to describe the dynamical behavior of the system in the form of some mathematical equations which is not necessarily of the linear nature [1]. Various sources of nonlinearities such as geometric nonlinearities, nonlinear materials, and nonlinear disturbing excitations are the primary sources of uncertainties that deteriorate the performance of mechanical structures. Hence, in order to reduce the uncertainties and in order to achieve robust structural configurations, particular attention has to be paid to the modelling of these nonlinearities [2–4]. The next step is then to handle the unwanted vibrations of a system by utilizing additional active elements which defines the concept

* Corresponding author.
E-mail addresses: atta.oveisi@rub.de, atta.oveisi@gmail.com (A. Oveisi), tamara.nestorovic@rub.de (T. Nestorović).

http://dx.doi.org/10.1016/j.cnsns.2016.09.012
1007-5704/

of adaptive mechanical systems. Such elements are realized by the multi-domain material-based transducers that simply enables the passive structure to react to the environmental inputs [5,6].

Furthermore, the current developments in robust control design for active structural dynamic control demand accurate uncertainty quantification [7]. For instance, in the state space modelling of nonlinear structures, $\dot{x} = \mathcal{A}x + \mathcal{B}u + \mathcal{G}$, where $\mathcal{A}, \mathcal{B}, x$ and u are respectively the state matrix, input matrix, state vector, and control input vector with appropriate dimensions, one possible form of including the modelling uncertainties is the lumped norm-bounded term $\mathcal{G}$. Such uncertainty quantification may include the unmodelled dynamics of nonlinear nature and obtaining an accurate estimation of H_∞-norm of $\mathcal{G}$ provides less conservative results in final closed-loop arrangement based on worst case analysis [8–10]. In application, very limited approaches are proposed for calculating the H_∞-norm of $\mathcal{G}$, however, with the method proposed in this paper and similar views for other geometries a good approximation is achievable [3]. This signifies the importance of current study.

The active vibration control is recognized to be effective especially in cases when the additional masses should be avoided, the system is highly nonlinear, and in the event of time-varying disturbance [11–13]. Piezo-transducers, due to their capability of coupling strain and electric field and due to the easiness of binding with the host structure, are the common candidates of active elements and therefore, a large number of researches are devoted in dynamic modelling of these structures [14–16]. Moita et al. used finite element method (FEM) to study the geometrical nonlinearity of thin laminated structures with embedded piezoelectric actuator/sensor elements [17]. Gao and Shen used active damping technique to control the nonlinear vibrations of smart structures. They employed the incremental FE equations using total Lagrange technique by utilizing virtual velocity incremental variation [18]. Belouettar et al. tackled the nonlinear vibration behavior of a smart beam under large deformation based on harmonic balance method. Their formulation included the implementation of a simple PD controller and the single-mode Galerkin method [19]. Ray and Shivakumar tackled the active constrained layer damping (ACLD) of geometrically nonlinear vibrations of laminated thin composite plates using piezoelectric fiber-reinforced composite (PFRC) materials [20]. Warminski et al. implemented different control algorithms on a nonlinear beam based on the model that they obtained using the Multiple Scale method [21]. In the second subsection of this paper, for the sake of completeness, a similar approach is combined with Galerkin technique to investigate the harmonic response of the geometrically nonlinear piezolaminated plate in frequency-domain. It should be mentioned that for the sake of brevity the sensitivity analyses are suppressed in this paper. Oveisi and Gudarzi studied the vibration control of a nonlinear plate using piezoelectric actuator based on an adaptive robust control algorithm. They evaluated the vibration suppression performance of the closed-loop system based on various control parameters, modelling uncertainty, and initial conditions [22]. They implemented an adaptive Ziegler Nichols PID (AZNPID) on a nonlinear beam and compared the vibration alleviation performance with the previous adaptive robust method [23]. Damanpack et al. studied the dynamic response of sandwich beams impacted by blast pulses with integrated piezoelectric sensor/actuator. They used von Karman theory and the first-order shear deformation theory to extract the nonlinear dynamics of the system [24].

To put in a nutshell, the following contributions are considered in this paper. First, Hamilton's principle is used to get the strong form of the nonlinear dynamical equation with the reflection of the second order strain terms by utilizing the von Karman strain-displacement correlation in form of an NPDE. Then, by introducing the proper and applicable feedback terms, the dynamic behavior of the open loop system is potentially enhanced in rejecting the possible mechanical disturbances. For this purpose and in order to identify the behavior of the closed-loop structure for various proportional and derivative gains, the obtained NPDE is first converted to a system of NODEs by employing Galerkin method and using the orthogonality of shape functions for simply supported boundary conditions. It should be pointed out that as long as the shape functions for a particular boundary condition are available, the current approach can be modified and then can be conducted to cover more general problem-specific boundary conditions. However, in this research, only the simply supported case is tackled. In the next step, the vibration attenuation and sensitivity of the dynamic response is assessed by variation of the controller gains and the magnitude of external disturbances. It is assumed that the plate is under large-amplitude vibration due to the existence of arbitrary mechanical disturbance. Moreover, to distinguish between attenuation performances of the closed-loop system in the case of static and dynamic loadings, the simulation examples are selected to cover both static and moving load with a complex profile. In the final section of the paper, some of the main observations are listed as conclusion.

2. Mathematical modelling

The sandwich piezolaminate plate, as shown in Fig. 1, consists of an elastic core, piezo-sensor layer, and piezo-actuator layer which are perfectly bonded on top and bottom of the core layer, respectively. Based on the Kirchhoff-Love plate theory, the displacement functions are described as

$$\begin{aligned} u(x,y,z,t) &= u_0(x,y,z,t) - z\frac{\partial w_0(x,y,t)}{\partial x}, \\ v(x,y,z,t) &= v_0(x,y,z,t) - z\frac{\partial w_0(x,y,t)}{\partial y}, \\ w(x,y,z,t) &= w_0(x,y,t), \end{aligned} \tag{1}$$

Considering the symmetricity of the general strain tensor and then applying the von Karman's theory for small strain and moderate rotation and neglecting all higher order terms except for $(\partial w/\partial x)^2$, $(\partial w/\partial y)^2$, and $(\partial w/\partial x)(\partial w/\partial y)$, the strain

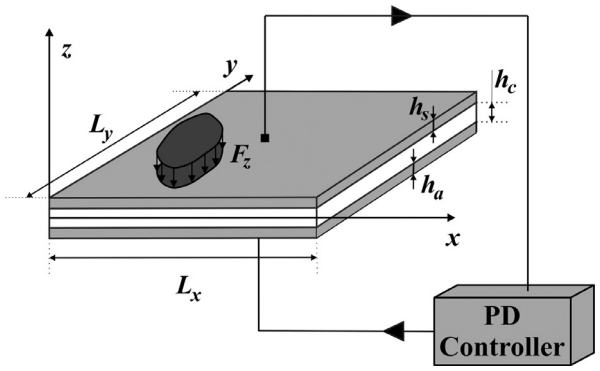

Fig. 1. Configuration of sandwich smart plate.

components can be obtained as

$$\varepsilon_{xx} = \varepsilon^0_{xx} + z\varepsilon^1_{xx}, \quad \varepsilon_{yy} = \varepsilon^0_{yy} + z\varepsilon^1_{yy}, \quad \varepsilon_{xy} = \varepsilon^0_{xy} + z\varepsilon^1_{xy}, \tag{2}$$

where,

$$\begin{aligned}
\varepsilon^0_{xx} &= \frac{\partial u_0}{\partial x} + \frac{1}{2}\left(\frac{\partial w_0}{\partial x}\right)^2, \quad \varepsilon^1_{xx} = -\frac{\partial^2 w_0}{\partial x^2},\\
\varepsilon^0_{yy} &= \frac{\partial u_0}{\partial y} + \frac{1}{2}\left(\frac{\partial w_0}{\partial y}\right)^2, \quad \varepsilon^1_{yy} = -\frac{\partial^2 w_0}{\partial y^2},\\
\varepsilon^0_{xy} &= \frac{1}{2}\left(\frac{\partial u_0}{\partial y} + \frac{\partial v_0}{\partial x} + \left(\frac{\partial w_0}{\partial x}\right)\left(\frac{\partial w_0}{\partial y}\right)\right), \quad \varepsilon^1_{xy} = -\frac{\partial^2 w_0}{\partial x \partial y}.
\end{aligned} \tag{3}$$

By assuming the polarization of both of the piezo-layers in z-direction, the constitutive equation of the piezoelectricity for orthotropic material and the case of plane strain can be written as [25]

$$\begin{Bmatrix} \sigma_{xx} \\ \sigma_{yy} \\ \sigma_{xy} \\ D_3 \end{Bmatrix} = \begin{bmatrix} c^{*i}_{11} & c^{*i}_{12} & 0 & -e^{*i}_{31} \\ c^{*i}_{11} & c^{*i}_{22} & 0 & -e^{*i}_{32} \\ 0 & 0 & c^{*i}_{66} & 0 \\ -e^{*i}_{31} & -e^{*i}_{32} & 0 & -e^{*i}_{33} \end{bmatrix} \begin{Bmatrix} \varepsilon_{xx} \\ \varepsilon_{yy} \\ \varepsilon_{xy} \\ E_3 \end{Bmatrix} \tag{4}$$

in which, σ_{kl}, (k, l=x, y), D_3, and E_3 are correspondingly the stress vector, electric displacement, and electric field in z-direction with i=s, a representing the sensor and actuator material properties with following definitions [26]

$$\begin{aligned}
c^{*i}_{11} &= c^i_{11} - \frac{{c^i_{13}}^2}{c^i_{33}}, \quad c^{*i}_{12} = c^i_{12} - \frac{c^i_{13}c^i_{23}}{c^i_{33}}, \quad c^{*i}_{22} = c^i_{22} - \frac{{c^i_{23}}^2}{c_{33}},\\
e^{*i}_{31} &= e^i_{31} - \frac{c^i_{13}e^i_{33}}{c^i_{33}}, \quad e^{*i}_{32} = e^i_{32} - \frac{c^i_{23}e^i_{33}}{c^i_{33}}, \quad \epsilon^{*i}_{33} = \epsilon^i_{33} + \frac{{e^i_{33}}^2}{c^i_{33}},
\end{aligned} \tag{5}$$

where $c^i_{\kappa\iota}$, $e^i_{\kappa\iota}(\kappa, \iota = 1, 2, 3)$, and ϵ_{33} are the components of elasticity-, piezoelectricity-tensor, and dielectric constant, respectively. The electrostatic equation ($\partial D_3/\partial z$=0), with zero electric displacement boundary conditions at both sides of piezo-layers results in $D(z) \equiv 0$ [19]. Considering ϕ as electrical potential and using Eq. (4) for electrical field together with $E_3(z)$=$-\partial\phi/\partial z$, one can obtain the electrical field of piezo-sensor layer as

$$E^s_3 = -\frac{\Delta\varphi_s}{h_s} - \frac{e^{*s}_{31}}{\epsilon^{*s}_{33}}(z - z_s)\varepsilon^1_{xx} - \frac{e^{*s}_{32}}{\epsilon^{*s}_{33}}(z - z_s)\varepsilon^1_{yy}, \tag{6}$$

where,

$$\Delta\varphi_s = \varphi_s = \frac{e^{*s}_{31}}{\epsilon^{*s}_{33}}h_s\left(\varepsilon^0_{xx} + z_s\varepsilon^1_{xx}\right) + \frac{e^{*s}_{32}}{\epsilon^{*s}_{33}}h_s\left(\varepsilon^0_{yy} + z_s\varepsilon^1_{yy}\right), \tag{7}$$

and z_s=$(h_c+h_s)/2$, z_a=$-(h_c+h_a)/2$, with h_s being the thickness of the piezo-sensor. For vibration control of the system, model-free PD feedback control law in terms of the measurement from sensor layer is incorporated within the dynamic modelling as $\varphi_a = G_p\varphi_s + G_d\dot{\varphi}_s$, where, G_p and G_d are the constant proportional and velocity feedback gains to be tuned, respectively.

3. Dynamic equation

The focal point of this paper is on utilizing Hamilton's principle in order to obtain the dynamic coupled equation of motion. The kinetic energy can be written as

$$K = \frac{1}{2}\int_V \left[\left(\frac{\partial u}{\partial t}\right)^2 + \left(\frac{\partial v}{\partial t}\right)^2 + \left(\frac{\partial w}{\partial t}\right)^2\right] dV, \tag{8}$$

where V and ρ are the volume and the density of the media, respectively. By taking variation of the kinetic energy with respect to the velocity vector and using Eq. (1), one can obtain

$$\delta K = \int_{\Omega_0} \left[I_0(\dot{u}_0\delta\dot{u}_0 + \dot{v}_0\delta\dot{v}_0 + \dot{w}_0\delta\dot{w}_0) - I_1\left(\dot{u}_0\frac{\partial\delta\dot{w}_0}{\partial x} + \delta\dot{u}_0\frac{\partial\dot{w}_0}{\partial x} + \dot{v}_0\frac{\partial\delta\dot{w}_0}{\partial y} + \delta\dot{v}_0\frac{\partial\dot{w}_0}{\partial y}\right) + I_2\left(\frac{\partial\dot{w}_0}{\partial x}\frac{\partial\delta\dot{w}_0}{\partial x} + \frac{\partial\dot{w}_0}{\partial y}\frac{\partial\delta\dot{w}_0}{\partial y}\right)\right] dxdy, \tag{9}$$

where Ω_0 is the area of the cross section parallel with oxy (see Fig. 1) and $I_j = \int_{-\frac{h}{2}}^{\frac{h}{2}} \rho z^j dz, \quad j = 0, 1, 2$ (Appendix A). I_1 represents the coupling effect between the axial and transverse vibration which is introduced by the piezoelectric layers. Strain energy can be written as

$$U = \frac{1}{2}\int_V (\sigma_{xx}\varepsilon_{xx} + \sigma_{yy}\varepsilon_{yy} + 2\sigma_{xy}\varepsilon_{xy}) dV, \tag{10}$$

by taking the variation of the strain energy (10) with respect to strain tensor and using Eqs. (2–4), Eq. (11) is formulated as

$$\delta U = \int_{\Omega_0} [N_{xx}\delta\varepsilon^0_{xx} + M_{xx}\delta\varepsilon^1_{xx} + N_{yy}\delta\varepsilon^0_{yy} + M_{yy}\delta\varepsilon^1_{yy} + 2N_{xy}\delta\varepsilon^0_{xy} + 2M_{xy}\delta\varepsilon^1_{xy}] dxdy, \tag{11}$$

where, $N_{kl} = \int_{-\frac{h}{2}}^{\frac{h}{2}} \sigma_{kl} dz$, and $M_{kl} = \int_{-\frac{h}{2}}^{\frac{h}{2}} z\sigma_{kl} dz$ (Appendix A). The variation of the external work due to the bending force $F_z(x, y, t)$ (see Fig. 1) can be calculated as

$$\delta W = \int_{\Omega_0} F_z \delta w_0 dxdy. \tag{12}$$

By applying Hamilton's principle to the piezo-plate, the time-dependent integral $\int_{t_1}^{t_2} (\delta K - \delta U + \delta W) dt = 0$ should be satisfied, in which, the effect of internal dielectric energy due to the boundary conditions for sensor and actuator layers is considered to be zero [27]. By taking the variation from the strain tensor (Eq. (2)) and substituting Eqs. (9,11, and 12) in the time-domain integral equation and then using integration by part technique, the following integral equation is attained

$$\int_{t_1}^{t_2} \left\{ \int_{\Omega_0} \left[-I_0(\ddot{u}_0\delta u_0 + \ddot{v}_0\delta v_0 + \ddot{w}_0\delta w_0) - I_1\left(\frac{\partial\ddot{u}_0}{\partial x}\delta w_0 - \frac{\partial\ddot{w}_0}{\partial x}\delta u_0 + \frac{\partial\ddot{v}_0}{\partial x}\delta w_0 - \frac{\partial\ddot{w}_0}{\partial x}\delta v_0\right) + I_2\left(\frac{\partial^2\ddot{w}_0}{\partial x^2}\delta w_0 + \frac{\partial^2\ddot{w}_0}{\partial y^2}\delta w_0\right) + \frac{\partial N_{xx}}{\partial x}\delta u_0 + \frac{\partial N_{yy}}{\partial y}\delta v_0 + \left(\frac{\partial N_{xx}}{\partial x}\frac{\partial w_0}{\partial x} + N_{xx}\frac{\partial^2 w_0}{\partial x^2} + \frac{\partial N_{yy}}{\partial y}\frac{\partial w_0}{\partial y} + N_{yy}\frac{\partial^2 w_0}{\partial y^2}\right)\delta w_0 + \left(\frac{\partial^2 M_{xx}}{\partial x^2} + \frac{\partial^2 M_{yy}}{\partial x^2}\right)\delta w_0 + \frac{\partial N_{xy}}{\partial y}\delta u_0 + \frac{\partial N_{xy}}{\partial x}\delta v_0 + \left(\frac{\partial N_{xy}}{\partial x}\frac{\partial w_0}{\partial y} + 2N_{xy}\frac{\partial^2 w_0}{\partial x\partial y} + \frac{\partial N_{xy}}{\partial y}\frac{\partial w_0}{\partial x}\right)\delta w_0 + 2\frac{\partial^2 M_{xy}}{\partial x\partial y}\delta w_0 + F_z\delta w_0 \right] dxdy \right\} dt. \tag{13}$$

Since in this paper the nonlinear transverse vibration of the smart sandwich plate is examined, the axial inertial terms are ignored and then by separating the coefficients of δu_0, δv_0, and δw_0 in integral Eq. (13) and setting them to zero individually, the following coupled nonlinear PDE in terms of lateral displacement can be written

$$I_1\frac{\partial\ddot{w}_0}{\partial x} + \frac{\partial N_{xx}}{\partial x} + \frac{\partial N_{xy}}{\partial y} = 0 \tag{14a}$$

$$I_1\frac{\partial\ddot{w}_0}{\partial y} + \frac{\partial N_{yy}}{\partial y} + \frac{\partial N_{xy}}{\partial x} = 0 \tag{14b}$$

$$-I_0\ddot{w}_0 + I_2\left(\frac{\partial^2\ddot{w}_0}{\partial x^2} + \frac{\partial^2\ddot{w}_0}{\partial y^2}\right) + \frac{\partial N_{xx}}{\partial x}\frac{\partial w_0}{\partial x} + N_{xx}\frac{\partial^2 w_0}{\partial x^2} + \frac{\partial N_{yy}}{\partial y}\frac{\partial w_0}{\partial y} + N_{yy}\frac{\partial^2 w_0}{\partial y^2} + \frac{\partial^2 M_{xx}}{\partial x^2} + \frac{\partial^2 M_{yy}}{\partial y^2} + \frac{\partial N_{xy}}{\partial x}\frac{\partial w_0}{\partial y} + 2N_{xy}\frac{\partial^2 w_0}{\partial x\partial y} + \frac{\partial N_{xy}}{\partial y}\frac{\partial w_0}{\partial x} + 2\frac{\partial^2 M_{xy}}{\partial x\partial y} + F_z = 0, \tag{14c}$$

by substituting Eqs. (14a, 14b) in Eq. (14c) and using the acquired results for the in-plane force resultants and moment resultants in Eq. (A.2–9), the final form of the dynamic equation of bending motion of the piezolaminated plate is obtained as

$$
\begin{aligned}
&-I_0\ddot{w}_0+I_2\left(\frac{\partial^2\ddot{w}_0}{\partial x^2}+\frac{\partial^2\ddot{w}_0}{\partial y^2}\right)-I_1\left(\frac{\partial\ddot{w}_0}{\partial x}\frac{\partial w_0}{\partial x}+\frac{\partial\ddot{w}_0}{\partial y}\frac{\partial w_0}{\partial y}\right)+\left[J_{xx1}\left(\frac{\partial w_0}{\partial x}\right)^2+J_{xx2}\frac{\partial^2 w_0}{\partial x^2}+J_{xx3}\left(\frac{\partial w_0}{\partial y}\right)^2+J_{xx4}\frac{\partial^2 w_0}{\partial y^2}\right.\\
&\left.+J_{xx5}\left(\frac{\partial w_0}{\partial x}\right)\left(\frac{\partial\dot{w}_0}{\partial x}\right)+J_{xx6}\frac{\partial^2\dot{w}_0}{\partial x^2}+J_{xx7}\left(\frac{\partial w_0}{\partial y}\right)\left(\frac{\partial\dot{w}_0}{\partial y}\right)+J_{xx8}\frac{\partial^2\dot{w}_0}{\partial y^2}\right]\left(\frac{\partial^2 w_0}{\partial x^2}\right)\\
&+\left[J_{yy1}\left(\frac{\partial w_0}{\partial x}\right)^2+J_{yy2}\frac{\partial^2 w_0}{\partial x^2}+J_{yy3}\left(\frac{\partial w_0}{\partial y}\right)^2+J_{yy4}\frac{\partial^2 w_0}{\partial y^2}+J_{yy5}\left(\frac{\partial w_0}{\partial x}\right)\left(\frac{\partial\dot{w}_0}{\partial x}\right)+J_{yy6}\frac{\partial^2\dot{w}_0}{\partial x^2}\right.\\
&\left.+J_{yy7}\left(\frac{\partial w_0}{\partial y}\right)\left(\frac{\partial\dot{w}_0}{\partial y}\right)+J_{yy8}\frac{\partial^2\dot{w}_0}{\partial y^2}\right]\left(\frac{\partial^2 w_0}{\partial y^2}\right)+2\left[J_{xy1}\left(\frac{\partial w_0}{\partial x}\right)\left(\frac{\partial w_0}{\partial y}\right)+J_{xy2}\frac{\partial^2 w_0}{\partial x\partial y}\right]\left(\frac{\partial^2 w_0}{\partial x\partial y}\right)\\
&+2K_{xx1}\left[\left(\frac{\partial^2 w_0}{\partial x^2}\right)^2+\left(\frac{\partial w_0}{\partial x}\right)\left(\frac{\partial^3 w_0}{\partial x^3}\right)\right]+K_{xx2}\frac{\partial^4 w_0}{\partial x^4}+2K_{xx3}\left[\left(\frac{\partial^2 w_0}{\partial x\partial y}\right)^2+\left(\frac{\partial w_0}{\partial y}\right)\left(\frac{\partial^3 w_0}{\partial x^2\partial y}\right)\right]\\
&+K_{xx4}\frac{\partial^4 w_0}{\partial x^2\partial y^2}+K_{xx5}\left[\left(\frac{\partial^3 w_0}{\partial x^3}\right)\left(\frac{\partial\dot{w}_0}{\partial x}\right)+2\left(\frac{\partial^2 w_0}{\partial x^2}\right)\left(\frac{\partial^2\dot{w}_0}{\partial x^2}\right)+\left(\frac{\partial^3\dot{w}_0}{\partial x^3}\right)\left(\frac{\partial w_0}{\partial x}\right)\right]\\
&+K_{xx6}\frac{\partial^4\dot{w}_0}{\partial x^4}+K_{xx7}\left[\left(\frac{\partial^3 w_0}{\partial x^2\partial y}\right)\left(\frac{\partial\dot{w}_0}{\partial y}\right)+2\left(\frac{\partial^2 w_0}{\partial x\partial y}\right)\left(\frac{\partial^2\dot{w}_0}{\partial x\partial y}\right)+\left(\frac{\partial^3\dot{w}_0}{\partial x^2\partial y}\right)\left(\frac{\partial w_0}{\partial y}\right)\right]+K_{xx8}\frac{\partial^4\dot{w}_0}{\partial x^2\partial y^2}\\
&+2K_{yy1}\left[\left(\frac{\partial^2 w_0}{\partial x\partial y}\right)^2+\left(\frac{\partial w_0}{\partial x}\right)\left(\frac{\partial^3 w_0}{\partial x\partial y^2}\right)\right]+K_{yy2}\frac{\partial^4 w_0}{\partial x^2\partial y^2}+2K_{yy3}\left[\left(\frac{\partial^2 w_0}{\partial y^2}\right)^2+\left(\frac{\partial w_0}{\partial y}\right)\left(\frac{\partial^3 w_0}{\partial y^3}\right)\right]\\
&+K_{yy4}\frac{\partial^4 w_0}{\partial y^4}+K_{yy5}\left[\left(\frac{\partial^3 w_0}{\partial x\partial y^2}\right)\left(\frac{\partial\dot{w}_0}{\partial x}\right)+2\left(\frac{\partial^2 w_0}{\partial x\partial y}\right)\left(\frac{\partial^2\dot{w}_0}{\partial x\partial y}\right)+\left(\frac{\partial^3\dot{w}_0}{\partial x\partial y^2}\right)\left(\frac{\partial w_0}{\partial x}\right)\right]\\
&+K_{yy6}\frac{\partial^4\dot{w}_0}{\partial x^2\partial y^2}+K_{yy7}\left[\left(\frac{\partial^3 w_0}{\partial y^3}\right)\left(\frac{\partial\dot{w}_0}{\partial y}\right)+2\left(\frac{\partial^2 w_0}{\partial y^2}\right)\left(\frac{\partial^2\dot{w}_0}{\partial y^2}\right)+\left(\frac{\partial^3\dot{w}_0}{\partial y^3}\right)\left(\frac{\partial w_0}{\partial y}\right)\right]+K_{yy8}\frac{\partial^4\dot{w}_0}{\partial y^4}\\
&+2K_{xy1}\left[\left(\frac{\partial^3 w_0}{\partial x^2\partial y}\right)\left(\frac{\partial w_0}{\partial y}\right)+\left(\frac{\partial^2 w_0}{\partial x^2}\right)\left(\frac{\partial^2 w_0}{\partial y^2}\right)+\left(\frac{\partial^2 w_0}{\partial x\partial y}\right)^2+\left(\frac{\partial w_0}{\partial x}\right)\left(\frac{\partial^3 w_0}{\partial x\partial y^2}\right)\right]+2K_{xy2}\frac{\partial^4 w_0}{\partial x^2\partial y^2}+F_z=0.
\end{aligned}
\tag{15}
$$

3.1. Time-domain analysis

For studying the transient response of the system, it is assumed that the structure is excited by a transversely distributed force $F_z=F_z(x, y, t)$. In order to solve Eq. (15), Galerkin approximation in spatial domain is adopted which transforms the nonlinear PDE of motion (15) into a system of nonlinear ODEs. For this purpose, the transverse deflection function by considering the simply support boundary conditions is defined as

$$
w_{0t}(x,y,t)=\sum_{i=1}^{\infty}\sum_{j=1}^{\infty}f_{ij}(t)\sin\left(\frac{i\pi x}{L_x}\right)\sin\left(\frac{j\pi y}{L_y}\right),
\tag{16}
$$

where i and j represent the mode number in x- and y-direction, respectively and subscript t stands for time-domain solution. $f_{ij}(t)$ represents the time-dependent unknown transient coefficients of the solution (16). Substituting Eq. (16) in Eq. (15), then using the orthogonality of mode-shapes, and finally after long mathematical manipulations, the system of nonlinear ODEs in Eq. (17) is resulted.

$$
\begin{aligned}
&c_1 f_{ij}(t)+f_{ij}(t)\sum_{\substack{n\\ n\neq i}}\sum_{\substack{m\\ m\neq j}}c_2 f_{nm}(t)+\sum_{\substack{n\\ n\neq i}}\sum_{\substack{m\\ m\neq j}}\sum_{\substack{k\\ k\neq i,n}}\sum_{\substack{l\\ l\neq j,m}}c_3 f_{nm}(t)f_{kl}(t)+c_4 f_{ij}^2(t)+\sum_{\substack{n\\ n\neq i}}\sum_{\substack{m\\ m\neq j}}c_5 f_{nm}^2(t)\\
&+c_6 f_{ij}^3(t)+c_7 f_{ij}^2(t)f'_{ij}(t)+f_{ij}\sum_{\substack{n\\ n\neq i}}\sum_{\substack{m\\ m\neq j}}c_8 f_{nm}^2(t)+c_9 f'_{ij}(t)+c_{10}f'_{ij}(t)f_{ij}(t)
\end{aligned}
$$

$$+ f'_{ij}(t) \sum_{\substack{n \\ n \neq i}} \sum_{\substack{m \\ m \neq j}} c_{11} f_{nm}(t) + f_{ij}(t) \sum_{\substack{n \\ n \neq i}} \sum_{\substack{m \\ m \neq j}} c_{12} f'_{nm}(t)$$
$$+ f_{ij}(t) \sum_{\substack{n \\ n \neq i}} \sum_{\substack{m \\ m \neq j}} c_{13} f'_{nm}(t) f_{nm}(t) + \sum_{\substack{n \\ n \neq i}} \sum_{\substack{m \\ m \neq j}} \sum_{\substack{k \\ k \neq i,n}} \sum_{\substack{l \\ l \neq j,m}} c_{14} f'_{nm}(t) f_{kl}(t)$$
$$+ \sum_{\substack{n \\ n \neq i}} \sum_{\substack{m \\ m \neq j}} c_{15} f'_{nm}(t) f_{nm}(t) + c_{16} f''_{ij}(t) + c_{17} f''_{ij}(t) f_{ij}(t)$$
$$+ f''_{ij}(t) \sum_{\substack{n \\ n \neq i}} \sum_{\substack{m \\ m \neq j}} c_{18} f_{nm}(t) + \sum_{\substack{n \\ n \neq i}} \sum_{\substack{m \\ m \neq j}} c_{19} f''_{nm}(t) f_{nm}(t)$$
$$+ \sum_{\substack{n \\ n \neq i}} \sum_{\substack{m \\ m \neq j}} \sum_{\substack{k \\ k \neq i,n}} \sum_{\substack{l \\ l \neq j,m}} c_{20} f''_{nm}(t) f_{kl}(t)$$
$$+ \int_0^{L_x} \int_0^{L_y} F_z(x,y,t) \sin\left(\frac{i\pi x}{L_x}\right) \sin\left(\frac{j\pi y}{L_y}\right) dx dy = 0, \tag{17}$$

where c_i, $i=1...20$ are given in Eq. (A.10). In order to obtain the transient response of the system for arbitrary external disturbance F_z and control gain (G_p, G_d) the built-in Mathematica function, "NDSolve" is used to solve the nonlinear system of ODEs (17).[1] In the sequel (Section 4), we shall present the numerical results in accordance with the numerical solution of NODEs (17).

3.2. Frequency-domain analysis

For studying the harmonic response of the system, it should be presumed that the structure is under the effect of a transverse harmonic force such as $F_z = f_z(x, y)\cos(\omega t)$ which is different than the general case introduced in Section 3.1. Accordingly, instead of the solution proposed in Eq. (16), based on the harmonic balance method [17,28], the solution for transverse vibration can be assumed as $w_{0f}(x,y,t) = (Ae^{i\omega t} + \bar{A}e^{-i\omega t})\sin(m\pi x/L_x)\sin(n\pi y/L_y)$, for the first harmonic (simply supported boundary condition). This converts the NPDE of motion of Eq. (15) to a new NODE. In such a solution, A represents the complex amplitude of the vibration to be calculated, $\bar{A}$ is the complex conjugate of A, and ω is the nonlinear vibration frequency. Next, in order to simplify the solution, the external force is assumed to be distributed on the upper layer uniformly ($F_z = Be^{i\omega t} + \bar{B}e^{-i\omega t}$) and it is assumed that $m=n=1$. As a result, substituting approximate solution of $w_{0f}(x,y,t)$ in dynamic equation of motion (Eq. (15)), using the orthogonality of the single shape function, and then setting the secular terms with $e^{i\omega t}$ factor, which represent resonance, equal to zero, gives the relation between the amplitude of single mode harmonic transverse vibration of the smart structure in terms of frequency of excitation. Since, the main goal of this paper is to give a semi-analytical solution for transient response of the piezo-laminated plates, the resulting nonlinear algebraic equation in frequency-domain is presented in Appendix B.

4. Numerical results

In this section, a parametric study is conducted to investigate the impact of various modelling parameters on the transient response of the system and stability of the closed-loop configuration. A Mathematica code is developed in the form of a Notebook file to compute the dynamic response of the coupled system. Numerical results are obtained based on the piezo-elasto-piezo plate that is depicted in Fig. 1. The host layer is a rectangular aluminum plate with $h_c = 0.003$ m, $L_x = 0.41$ m, $L_y = 0.386$ m, and $\rho_c = 2700$ kg/m^3. The sensor and the actuator layers are respectively assumed to be perfectly bonded on the upper and lower surfaces of the host layer ($h_a = h_c = 0.0005$ m) and fabricated from PZT4/$Ba_2NaNb_5O_{15}$ with $\rho_a = 5300$ kg/m^3 and $\rho_s = 7500$ kg/m^3. All other material properties are given in Table 1.

In order to distinguish between the performance of the controller in suppressing the nonlinear vibration, two kinds of loadings are considered in the simulation results. The first one is a static point force on the top surface of the plate (load 1 in Fig. 2) and the second one is the moving concentrated force along the second order trajectory (load 2 in Fig. 2). In different simulation examples, especially for open loop configuration, the location of the static concentrated force is selected both geometrically symmetrical and non-symmetrical. This gives a better view of the system behavior. Additionally, Load 2 in Fig. 2 is chosen to include two phases of loading and unloading (relaxation) to investigate the performance of the control system in rejecting the disturbance both in transient period as well as the steady state response.

The sensitivity of the open loop transient response under a point force excitation with the amplitude of 10^4 N at $x_0 = L_x/8$, $y_0 = L_y/8$ is investigated in Fig. 3. This figure shows the displacement of the center of the smart plate. In order to alleviate the

[1] The authors are willing to share their script in the form of Notebook file (.nb) compatible with Wolfram Mathematica with the interested reader.

Table 1
Material properties of each layer of sandwich plate.

	Actuator layer	Sensor layer	Host layer
$c_{ij}(\mathrm{N/m^2})$			
c_{11}	23.9×10^{10}	13.9×10^{10}	11.2×10^{10}
c_{12}	10.4×10^{10}	7.8×10^{10}	6.04×10^{10}
c_{12}	5.2×10^{10}	7.43×10^{10}	6.04×10^{10}
c_{22}	24.7×10^{10}	13.9×10^{10}	11.2×10^{10}
c_{23}	5.2×10^{10}	7.43×10^{10}	6.04×10^{10}
c_{33}	13.5×10^{10}	11.5×10^{10}	11.2×10^{10}
c_{44}	6.5×10^{10}	2.56×10^{10}	2.59×10^{10}
c_{55}	6.6×10^{10}	2.56×10^{10}	2.59×10^{10}
c_{66}	7.6×10^{10}	3.06×10^{10}	2.59×10^{10}
$e_{ij}(\mathrm{C/m^2})$			
e_{15}	2.8	12.7	
e_{24}	3.4	12.7	
e_{31}	− 0.4	− 5.2	
e_{32}	− 0.3	− 5.2	
e_{33}	4.3	15.1	
$\varepsilon_{ij}(\mathrm{F/m})$			
ε_{11}	196×10^{-11}	650×10^{-11}	
ε_{22}	201×10^{-11}	650×10^{-11}	
ε_{33}	28×10^{-11}	560×10^{-11}	

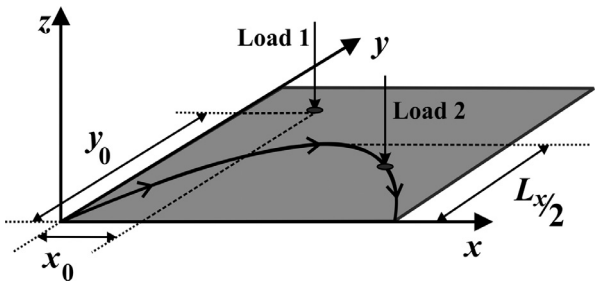

Fig. 2. The two external applied disturbance on the top surface of the plate.

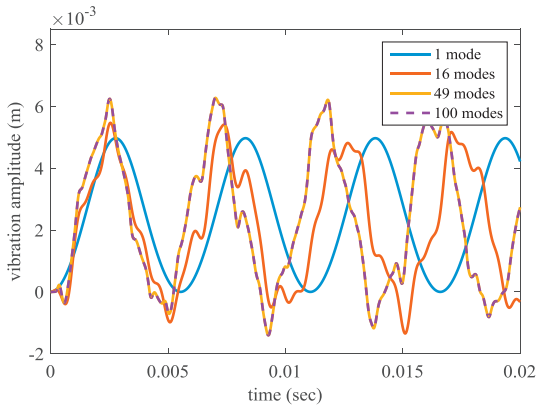

Fig. 3. Sensitivity of the solution to the number of shape functions that are included in the Galerkin method for simply supported case under point loading.

computational burden of the numerical solution of Eq. (17) the minimum number of required shape functions is determined. Accordingly, it can be seen that, for static point force at least 49 terms are required to guarantee the convergence of the response to a single transient response. It should be mentioned that, the response of the system by assuming single mode plant cannot describe the time-dependent behavior of the system which is tackled by Belouettar et al. for simply supported beam [19].

In order to study the effectiveness of the feedback control system, the transient response of the system is compared for various values of the proportional and derivative gain (G_p and G_d). For this purpose, the linear form of Eq. (17) is obtained by setting all high order terms equal to zero. All of the remaining linear terms are considered as the dynamics of the open loop system.

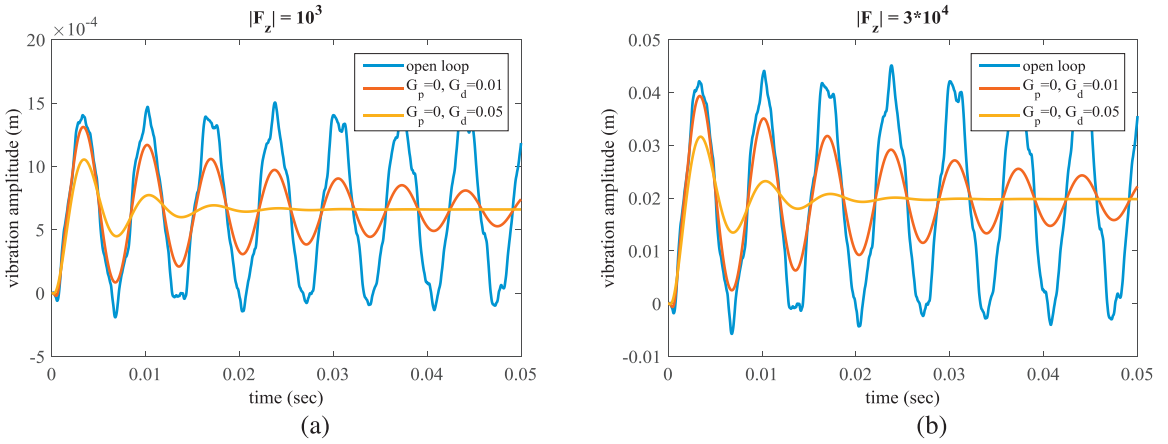

Fig. 4. Vibration amplitude of the linear controlled system under excitation force with two different magnitudes.

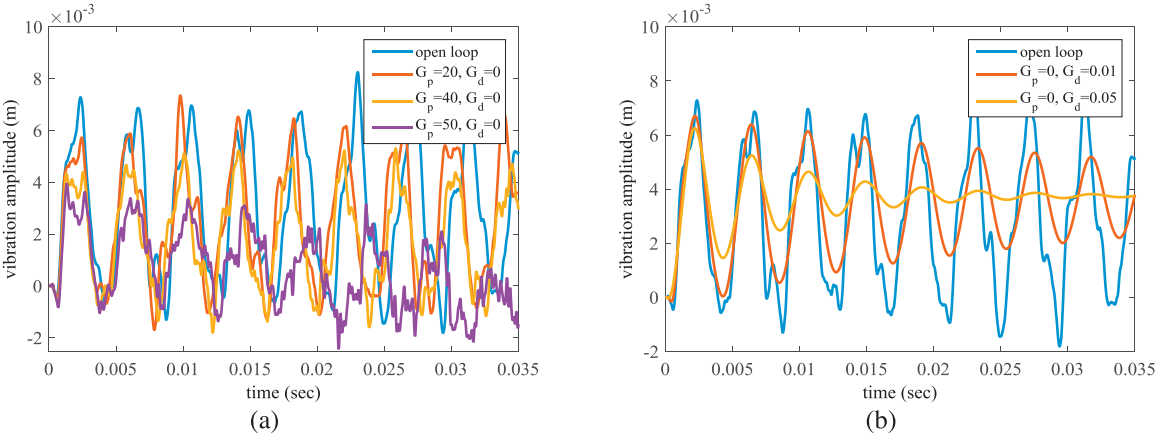

Fig. 5. Effectiveness of the vibration control system in suppressing the vibration.

Next, to investigate the effect of excitation amplitude as well as control parameter (G_d) in a representation independent from the nature of the force, a static point force at $x_0 = L_x/5$, $y_0 = L_y/5$ is applied on the system for two different values of the excitation magnitude as depicted in Fig. 4a and b. Fig. 4 shows that in contrast to the nonlinear case, this system has a linear relation between the excitation and vibration amplitude. In addition, the vibration suppression performance is independent of magnitude of the excitation which is less realistic and this emphasizes the importance of this study.

The nonlinear vibration control of the sandwich plate ($|F_z| = 10^4$) is studied in Fig. 5. This figure consists of two sub-plots in which the effect of the proportional and derivative gains are studied individually due to the nonlinear nature of the problem. In the first sub-plot (Fig. 5a), although increasing G_p attenuates the vibration amplitude, it also increases the frequency of the vibration. This is due to the fact that the proportional gain of the feedback channel can change the global stiffness of the structure (see Eq. (17) and c_1 in Eq. (A10)). In contrast to the linear case and owing to higher order coupled strain term, the closed-loop system is highly sensitive with respect to G_p and increasing proportional gain $G_p > 40$ in our simulations, leads to performance degradation and then instability. However, increasing G_d similar to the linear behavior improves the settling time and stability of the system (see Fig. 5b). Moreover, it can be seen in Fig. 5b that the derivative term of the controller can reject the higher order terms.

Fig. 6 displays the time series of snap-shots of displacement propagation in the piezolaminated sandwich plate under mechanical loading at $x_0 = L_x/5$, $y_0 = L_y/5$.

Regions having lower vibrating levels are depicted in darker colors. These figures are obtained by setting the magnitude of the external input, the proportional, and the derivative gain equal to 10^5, 25, and 0.001, respectively. Fig. 6 shows that, since the external force continues to act on the coupled structure, although the feedback control system attenuates the transient part of the vibration, the static displacement remains mostly uncontrolled.

In order to investigate the performance of the control system after removing the force from the structure (relaxation phase), the moving concentrated load $F_z(x, y, t) = F_0\delta(x - \frac{L_x}{t_0}t)\delta(y + \frac{2L_y}{t_0^2}t^2 - \frac{2L_y}{t_0}t)[H(t) - H(t - t_0)]$ is applied as the exogenous time-varying disturbance in time interval $[0\, t_0]$ sec on second order trajectory (see Fig. 2). In this function, $\delta(.)$ and $H(.)$ stand for the Dirac's delta and Heaviside step functions, respectively. Because of the nonlinearity of the problem, a similar

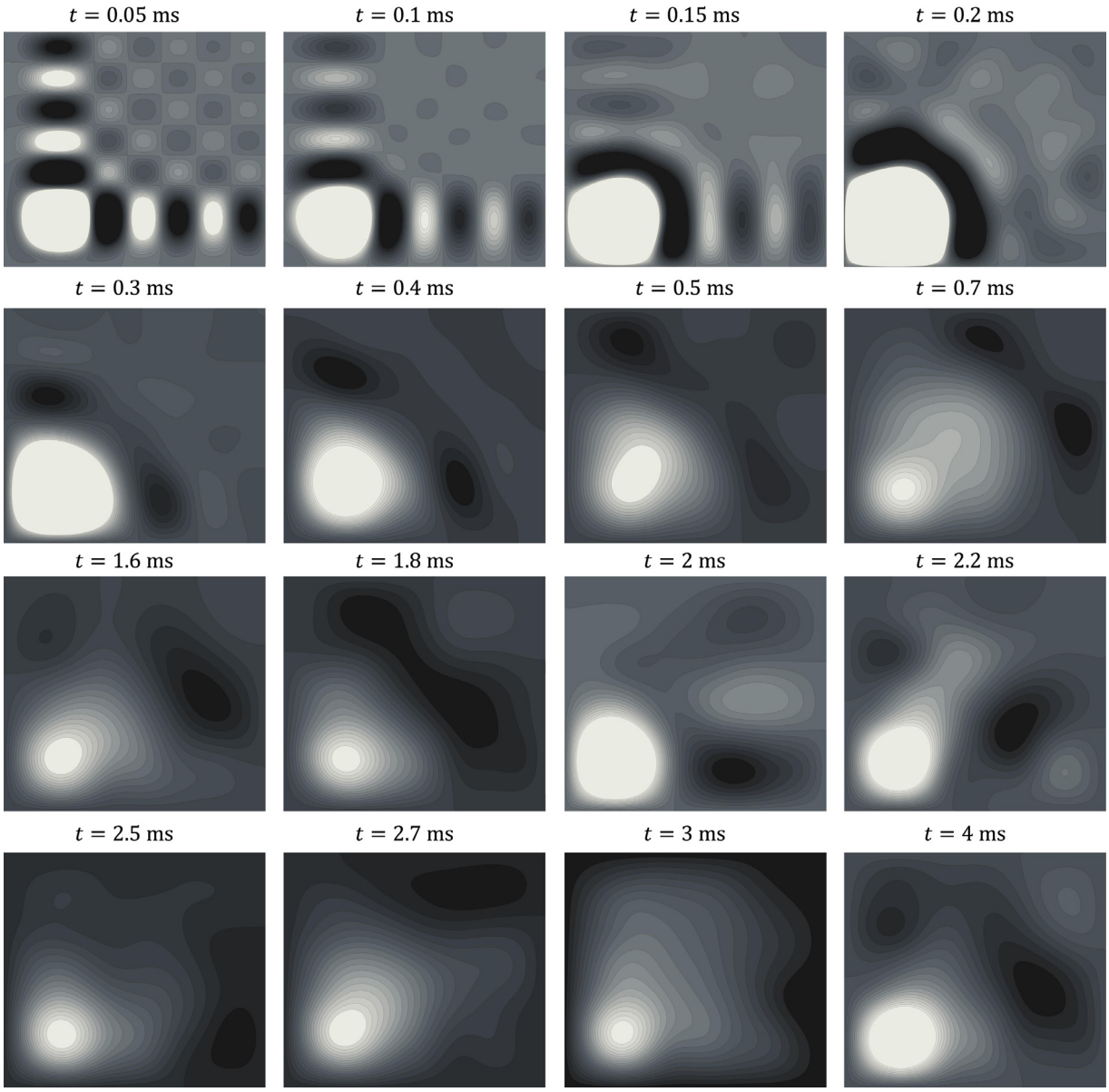

Fig. 6. Time snap-shots of the vibration propagation in the piezoelectric laminated plate due to the mechanical point load.

analysis to Fig. 3 is conducted to determine the minimum required number of shape functions in Galerkin method that satisfies the convergence, and the first 100 mode-shapes of the coupled piezolaminated structure are taken as the plant model. Fig. 7 illustrates the dynamic response of the system under moving load on a second order profile that is depicted in Fig. 2. The loading phase lasts 0.05 sec during which the concentrated force reaches $x=L_x/2$ and $y=L_y/2$ at $t_0=0.025$ sec. The control system is unable to damp the static deformation of the structure during the loading phase, however, it can be seen that the oscillations around the static deflection is suppressed by activating the PD control in feedback channel. In addition, by comparing two controlled outputs, it is obvious that the undershoot of the closed-loop system with $G_p=40$ is more than in the case with $G_p=10$ which is the price for decreasing the steady state error.

Finally, In order to validate the proposed analytical model in this paper, the six fundamental natural frequencies of the system are compared with results calculated by means of the commercial finite element package. The results, as shown in Table 2, demonstrate very good agreements with those obtained from ABAQUS.

The magnitude of FRF of the sandwich piezolaminated plate based on the proposed model in this paper is compared with the result that is obtained from ABAQUS by steady-state dynamic, Direct method within the frequency range of [100 420] Hz as shown in Fig. 8. The FRF of the system is obtained by exciting the plate with a harmonic constant point force at $x_0=3L_x/4$ and $y_0=L_y/4$ and collecting the response of the system at the nodal point of $x_1=L_x/4$ and $y_1=3L_y/4$. The

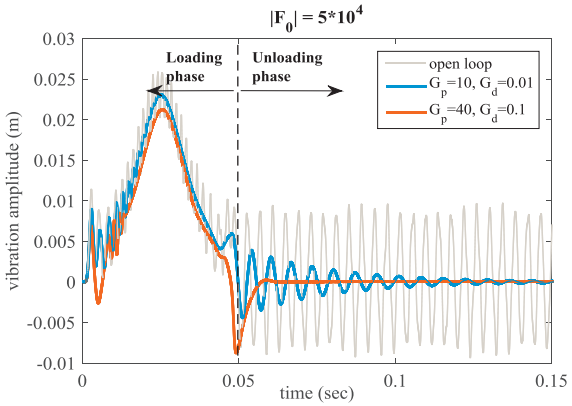

Fig. 7. Transient response of system under moving load.

Table 2
Comparison of the six fundamental natural frequencies of the coupled structure (Hz).

Method	Mode number					
	(1,1)	(2,1)	(1,2)	(2,2)	(3,1)	(1,3)
Present	147.54	343.39	392.35	589.92	668.72	799.45
FEM	146.90	342.44	390.83	586.53	667.40	796.15
Error (%)	0.43	0.28	0.39	0.57	0.20	0.41

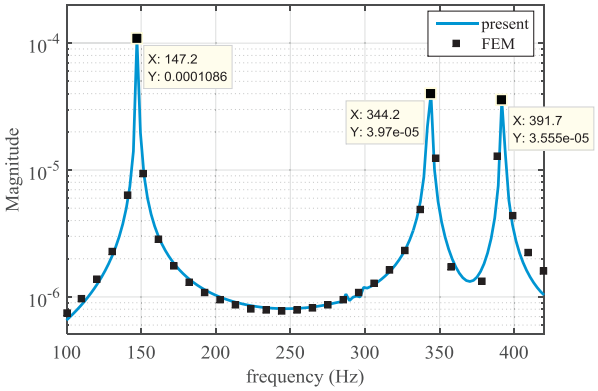

Fig. 8. FRF of the sandwich plate under a point force at $x_0 = 3L_x/4$, $y_0 = L_y/4$.

analytical solution is carried out by taking fast Fourier transformation (FFT) from the transient response of the analytical model under the same excitation.

In order to validate the analytical model in time-domain, dynamic explicit analysis is performed in FE package (ABAQUS) under a point force excitation that acts at the center of the plate with a transient form of $t/t_0(U(t)-U(t-t_0))+(-t/t_0+2)(U(t-t_0)-U(t-t_1))$ with $t_0 = 1e^{-4}$ sec and $t_1 = 2e^{-4}$ sec and $U(.)$ being the step function. The results for the deformation of the piezolaminated plate are shown in two different time steps in Fig. 9[2].

Moreover, for the same loading as in Fig. 9, the amplitude of vibrations in transverse direction based on the proposed method are compared with the solution of FE package (ABAQUS). Due to long simulation that is required by ABAQUS, the results are presented only for 10 ms in Fig. 10.

Remark 1. It should be pointed out that in an analogy between the proposed semi-analytical solution and the FE approach, the parameters that control the convergence of the solution are respectively the number of terms included in Galerkin spatial counterpart and the mesh density in FE solution. Since the convergence analysis for proposed solution is presented in Fig. 3, the mesh convergence analysis is essential for the results in Figs. 8 and 9. Accordingly, after mesh convergence analysis in the ABAQUS model, 113,160 twenty-node quadratic piezoelectric brick (C3D20RE) elements were

[2] The interested reader may contact the corresponding author to obtain the .cae and .jnl files of ABAQUS simulations.

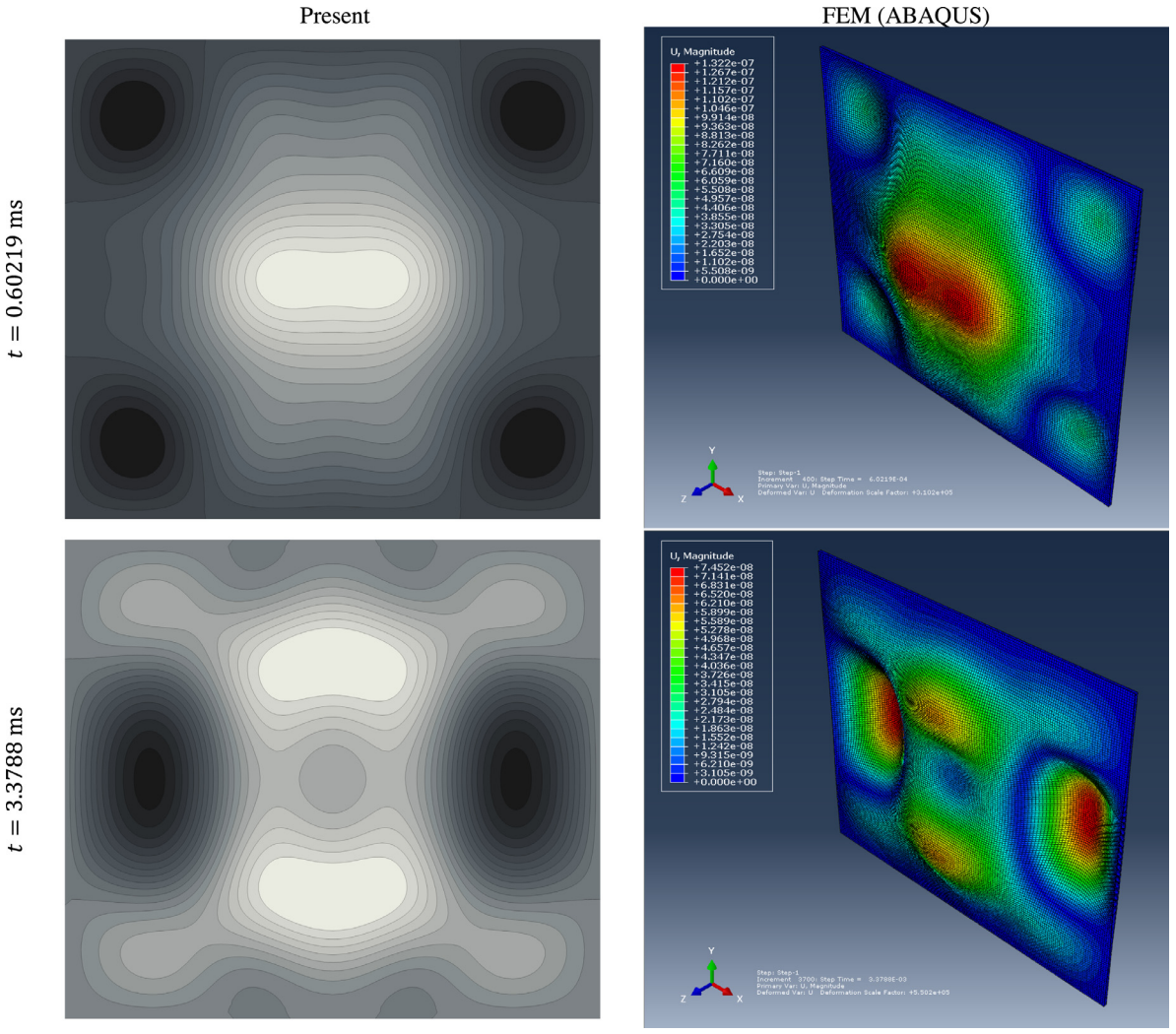

Fig. 9. Validation of the deformation of the coupled plate with FEM (spatial-domain).

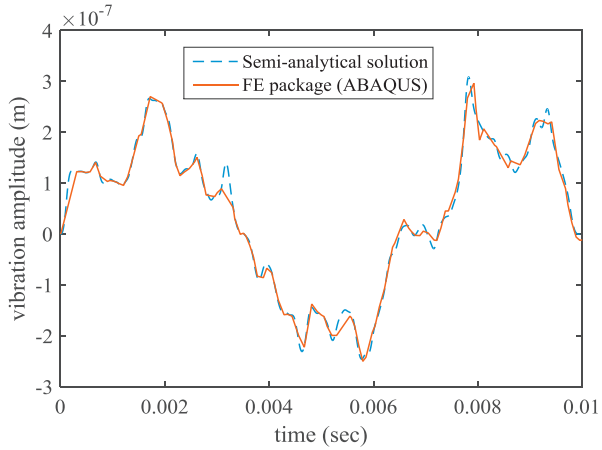

Fig. 10. Validating the vibration amplitude in time-domain.

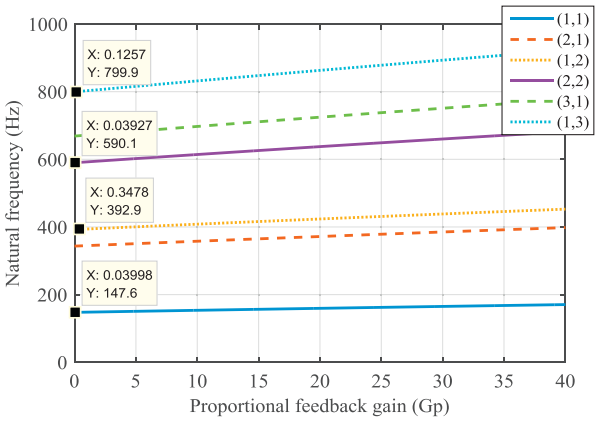

Fig. 11. Influence of the proportional gain of six fundamental natural frequencies.

employed as meshing configuration for the sensor and actuator layers, and 226,320 twenty-node quadratic brick (C3D20R) elements were used to model the host structure. For the sake of brevity, these analyses are not reported in the paper.

Finally, by aiming at evaluating the influence of proportional gain (G_p) on the fundamental natural frequencies of the system (one to six) in free vibration, the nonlinear terms are set to zero and the linear natural frequencies are calculated ($\sqrt{K^R/M}$) while sweeping the proportional gain of the model-free PD controller (see Appendix B). It is observed that by increasing the proportional gain (G_p), the natural frequencies of the system tend to increase (see Fig. 11). This is due to the fact that the proportional term of the feedback channel changes the global stiffness of the system drastically and similar behavior was observed in Fig. 5a. Additionally, when $G_p=0$, the results (see datatips in Fig. 11) are in agreement with those presented in Table 2. The legend of Fig. 11, similar to Table. 2 is written in terms of modal numbers is x- and y-directions (m, n) for the first six fundamental natural frequencies.

5. Conclusion

A new analytical formulation is developed for predicting the nonlinear dynamic behavior of composite piezolaminated plate for simply supported boundary conditions. Accordingly, some important aspects of this contribution are listed as:

- The equation of motion of the coupled electro-mechanical system is derived considering the geometrical nonlinearities (strain-displacement relationship of von Karman type) and satisfying the appropriate electrostatic piezo-sensor/-actuator boundary conditions.
- Hamilton's principle is used to extract the strong form of the equation of motion in the form of an NPDE.
- Galerkin method and orthogonality of shape functions for simply supported boundary conditions in spatial domain are employed and then the obtained nonlinear system of ODEs of motion is solved numerically.
- Vibration suppression problem is investigated by the implementation of a model-free control law.
- The presented method as a semi-analytical approach is much faster than FE package ABAQUS and, therefore, it can be used as a benchmark in designing smart plates under large vibration amplitude.
- High order strain terms play an important role in the dynamic response of the closed-loop system, and the presented model shows much realistic results for vibration control compared to the linear simplification. Two important observation compared to classical linear assumptions are 1) The sensitivity of the transient behavior of the structure to the magnitude of the excitation in large vibration amplitudes. 2) Identifying the realistic bounds of proportional feedback gain that may result in structural instability.
- The proposed method is not limited to simply supported boundary conditions as long as the appropriate shape functions in the Galerkin approach is available to solve the partial differential equation in the spatial domain. However, regarding the interaction of the host and piezo-layers such as imperfect bonding conditions further analysis are required which is out of the scope of this paper.
- The semi-analytical solution can handle arbitrary mechanical loading such as moving load (see Fig. 7) and accordingly the effect of arbitrary elastic foundations can also be realized from this channel.

Appendix A

The constants in Eq. (9) are calculated as

$$I_0 = h_a\rho_a + h_c\rho_c + h_s\rho_s,$$
$$I_1 = h_a z_a\rho_a + h_s z_s\rho_s,$$
$$I_2 = \frac{h_a^3\rho_a}{12} + \frac{h_c^3\rho_c}{12} + \frac{h_s^3\rho_s}{12} + \rho_a h_a z_a^2 + \rho_s h_s z_s^2. \tag{A.1}$$

By employing the definition of N_{xx} for the coupled three layered media, we can write

$$N_{xx} = \int_{-h/2}^{h/2} \sigma_{xx} dz = \int_c \sigma_{xx} dz + \int_s \sigma_{xx} dz + \int_a \sigma_{xx} dz, \tag{A.2}$$

then, using Eqs. (2) and (4) and carrying out the integration in z-direction the following equation can be obtained

$$\begin{aligned} N_{xx} = {} & J_{xx1}\left(\frac{\partial w_0}{\partial x}\right)^2 + J_{xx2}\frac{\partial^2 w_0}{\partial x^2} + J_{xx3}\left(\frac{\partial w_0}{\partial y}\right)^2 + J_{xx4}\frac{\partial^2 w_0}{\partial y^2} + J_{xx5}\left(\frac{\partial w_0}{\partial x}\right)\left(\frac{\partial \dot{w}_0}{\partial x}\right) + J_{xx6}\frac{\partial^2 \dot{w}_0}{\partial x^2} \\ & + J_{xx7}\left(\frac{\partial w_0}{\partial y}\right)\left(\frac{\partial \dot{w}_0}{\partial y}\right) + J_{xx8}\frac{\partial^2 \dot{w}_0}{\partial y^2}, \end{aligned} \tag{A.4}$$

and similarly

$$\begin{aligned} N_{yy} = {} & J_{yy1}\left(\frac{\partial w_0}{\partial x}\right)^2 + J_{yy2}\frac{\partial^2 w_0}{\partial x^2} + J_{yy3}\left(\frac{\partial w_0}{\partial y}\right)^2 + J_{yy4}\frac{\partial^2 w_0}{\partial y^2} + J_{yy5}\left(\frac{\partial w_0}{\partial x}\right)\left(\frac{\partial \dot{w}_0}{\partial x}\right) + J_{yy6}\frac{\partial^2 \dot{w}_0}{\partial x^2} \\ & + J_{yy7}\left(\frac{\partial w_0}{\partial y}\right)\left(\frac{\partial \dot{w}_0}{\partial y}\right) + J_{yy8}\frac{\partial^2 \dot{w}_0}{\partial y^2}, \end{aligned} \tag{A.5}$$

$$N_{xy} = J_{xy1}\left(\frac{\partial w_0}{\partial x}\right)\left(\frac{\partial w_0}{\partial y}\right) + J_{xy2}\frac{\partial^2 w_0}{\partial x \partial y}, \tag{A.6}$$

$$\begin{aligned} M_{xx} = {} & K_{xx1}\left(\frac{\partial w_0}{\partial x}\right)^2 + K_{xx2}\frac{\partial^2 w_0}{\partial x^2} + K_{xx3}\left(\frac{\partial w_0}{\partial y}\right)^2 + K_{xx4}\frac{\partial^2 w_0}{\partial y^2} + K_{xx5}\left(\frac{\partial w_0}{\partial x}\right)\left(\frac{\partial \dot{w}_0}{\partial x}\right) + K_{xx6}\frac{\partial^2 \dot{w}_0}{\partial x^2} \\ & + K_{xx7}\left(\frac{\partial w_0}{\partial y}\right)\left(\frac{\partial \dot{w}_0}{\partial y}\right) + K_{xx8}\frac{\partial^2 \dot{w}_0}{\partial y^2}, \end{aligned} \tag{A.7}$$

$$\begin{aligned} M_{yy} = {} & K_{yy1}\left(\frac{\partial w_0}{\partial x}\right)^2 + K_{yy2}\frac{\partial^2 w_0}{\partial x^2} + K_{yy3}\left(\frac{\partial w_0}{\partial y}\right)^2 + K_{yy4}\frac{\partial^2 w_0}{\partial y^2} + K_{yy5}\left(\frac{\partial w_0}{\partial x}\right)\left(\frac{\partial \dot{w}_0}{\partial x}\right) + K_{yy6}\frac{\partial^2 \dot{w}_0}{\partial x^2} \\ & + K_{yy7}\left(\frac{\partial w_0}{\partial y}\right)\left(\frac{\partial \dot{w}_0}{\partial y}\right) + K_{yy8}\frac{\partial^2 \dot{w}_0}{\partial y^2}, \end{aligned} \tag{A.8}$$

$$M_{xy} = K_{xy1}\left(\frac{\partial w_0}{\partial x}\right)\left(\frac{\partial w_0}{\partial y}\right) + K_{xy2}\frac{\partial^2 w_0}{\partial x \partial y}, \tag{A.9}$$

where,

$$J_{xx1} = \frac{1}{2}\left[c_{11}^c h_c + c_{11}^{*s} h_s + c_{11}^{*a} h_a + (e_{31}^{*s} - G_p e_{31}^{*a})\frac{e_{31}^{*s}}{\epsilon_{33}^{*s}} h_s\right],$$

$$J_{xx2} = -\left[c_{11}^{*s} h_s z_s + c_{11}^{*a} h_a z_a + (e_{31}^{*s} - G_p e_{31}^{*a})\frac{e_{31}^{*s}}{\epsilon_{33}^{*s}} h_s z_s\right],$$

$$J_{xx3} = \frac{1}{2}\left[c_{12}^c h_c + c_{12}^{*s} h_s + c_{12}^{*a} h_a + (e_{31}^{*s} - G_p e_{31}^{*a})\frac{e_{32}^{*s}}{\epsilon_{33}^{*s}} h_s\right],$$

$$J_{xx4} = -\left[c_{12}^{*s} h_s z_s + c_{12}^{*a} h_a z_a + (e_{31}^{*s} - G_p e_{31}^{*a})\frac{e_{32}^{*s}}{\epsilon_{33}^{*s}} h_s z_s\right],$$

$$J_{xx5} = -\frac{e_{31}^{*a} e_{31}^{*s}}{\epsilon_{33}^{*s}} G_d h_s,$$

$$J_{xx6} = -\frac{e_{31}^{*a} e_{31}^{*s}}{\epsilon_{33}^{*s}} G_d h_s z_s,$$

$$J_{xx7} = -\frac{e_{31}^{*a} e_{32}^{*s}}{\epsilon_{33}^{*s}} G_d h_s,$$

$$J_{xx8} = -\frac{e_{31}^{*a} e_{32}^{*s}}{\epsilon_{33}^{*s}} G_d h_s z_s,$$

$$J_{yy1} = \frac{1}{2}\left[c_{12}^{c}h_c + c_{12}^{*s}h_s + c_{12}^{*a}h_a + (e_{32}^{*s} - G_p e_{32}^{*a})\frac{e_{31}^{*s}}{\epsilon_{33}^{*s}}h_s\right],$$

$$J_{yy2} = -\left[c_{12}^{*s}h_s z_s + c_{12}^{*a}h_a z_a + (e_{32}^{*s} - G_p e_{32}^{*a})\frac{e_{31}^{*s}}{\epsilon_{33}^{*s}}h_s z_s\right],$$

$$J_{yy3} = \frac{1}{2}\left[c_{22}^{c}h_c + c_{22}^{*s}h_s + c_{22}^{*a}h_a + (e_{32}^{*s} - G_p e_{32}^{*a})\frac{e_{32}^{*s}}{\epsilon_{33}^{*s}}h_s\right],$$

$$J_{yy4} = -\left[c_{22}^{*s}h_s z_s + c_{22}^{*a}h_a z_a + (e_{32}^{*s} - G_p e_{32}^{*a})\frac{e_{32}^{*s}}{\epsilon_{33}^{*s}}h_s z_s\right],$$

$$J_{yy5} = -\frac{e_{32}^{*a}e_{31}^{*s}}{\epsilon_{33}^{*s}}G_d h_s,$$

$$J_{yy6} = -\frac{e_{32}^{*a}e_{31}^{*s}}{\epsilon_{33}^{*s}}G_d h_s z_s,$$

$$J_{yy7} = -\frac{e_{32}^{*a}e_{32}^{*s}}{\epsilon_{33}^{*s}}G_d h_s,$$

$$J_{yy8} = -\frac{e_{32}^{*a}e_{32}^{*s}}{\epsilon_{33}^{*s}}G_d h_s z_s,$$

$$J_{xy1} = \frac{1}{2}[2c_{66}^{c}h_c + 2c_{66}^{*s}h_s + 2c_{66}^{*a}h_a],$$

$$J_{xy2} = -[2c_{66}^{*s}h_s z_s + 2c_{66}^{*a}h_a z_a],$$

$$K_{xx1} = \frac{1}{2}\left[c_{11}^{*s}h_s z_s + c_{11}^{*a}h_a z_a + (e_{31}^{*s}z_s - G_p e_{31}^{*a}z_a)\frac{e_{31}^{*s}}{\epsilon_{33}^{*s}}h_s\right],$$

$$K_{xx2} = -\left[\frac{1}{12}c_{11}^{c}h_c^3 + c_{11}^{*s}\left(z_s^2 h_s + \frac{1}{12}h_s^3\right) + c_{11}^{*a}\left(z_a^2 h_a + \frac{1}{12}h_a^3\right) + (e_{31}^{*s}z_s - G_p e_{31}^{*a}z_a)\frac{e_{31}^{*s}}{\epsilon_{33}^{*s}}h_s z_s + \left(\frac{h_s^3}{12}\frac{\left(e_{31}^{*s}\right)^2}{\epsilon_{33}^{*s}} + \frac{h_a^3}{12}\frac{\left(e_{31}^{*a}\right)^2}{\epsilon_{33}^{*a}}\right)\right],$$

$$K_{xx3} = \frac{1}{2}\left[c_{12}^{*s}h_s z_s + c_{12}^{*a}h_a z_a + (e_{31}^{*s}z_s - G_p e_{31}^{*a}z_a)\frac{e_{32}^{*s}}{\epsilon_{33}^{*s}}h_s\right],$$

$$K_{xx4} = -\left[\frac{1}{12}c_{12}^{c}h_c^3 + c_{12}^{*s}\left(z_s^2 h_s + \frac{1}{12}h_s^3\right) + c_{12}^{*a}\left(z_a^2 h_a + \frac{1}{12}h_a^3\right) + (e_{31}^{*s}z_s - G_p e_{31}^{*a}z_a)\frac{e_{32}^{*s}}{\epsilon_{33}^{*s}}h_s z_s + \left(\frac{h_s^3}{12}\frac{e_{31}^{*s}e_{32}^{*s}}{\epsilon_{33}^{*s}} + \frac{h_a^3}{12}\frac{e_{31}^{*a}e_{32}^{*a}}{\epsilon_{33}^{*a}}\right)\right],$$

$$K_{xx5} = -\frac{e_{31}^{*a}e_{31}^{*s}}{\epsilon_{33}^{*s}}G_d h_s z_a,$$

$$K_{xx6} = -\frac{e_{31}^{*a}e_{31}^{*s}}{\epsilon_{33}^{*s}}G_d h_s z_s z_a,$$

$$K_{xx7} = -\frac{e_{31}^{*a}e_{32}^{*s}}{\epsilon_{33}^{*s}}G_d h_s z_a,$$

$$K_{xx8} = -\frac{e_{31}^{*a}e_{32}^{*s}}{\epsilon_{33}^{*s}}G_d h_s z_s z_a,$$

$$K_{yy1} = \frac{1}{2}\left[c_{12}^{*s}h_s z_s + c_{12}^{*a}h_a z_a + (e_{32}^{*s}z_s - G_p e_{32}^{*a}z_a)\frac{e_{31}^{*s}}{\epsilon_{33}^{*s}}h_s\right],$$

$$K_{yy2} = -\left[\frac{1}{12}c_{12}^{c}h_c^3 + c_{12}^{*s}\left(z_s^2 h_s + \frac{1}{12}h_s^3\right) + c_{12}^{*a}\left(z_a^2 h_a + \frac{1}{12}h_a^3\right) + (e_{32}^{*s}z_s - G_p e_{32}^{*a}z_a)\frac{e_{31}^{*s}}{\epsilon_{33}^{*s}}h_s z_s + \left(\frac{h_s^3}{12}\frac{e_{31}^{*s}e_{32}^{*s}}{\epsilon_{33}^{*s}} + \frac{h_a^3}{12}\frac{e_{31}^{*a}e_{32}^{*a}}{\epsilon_{33}^{*a}}\right)\right],$$

$$K_{yy3} = \frac{1}{2}\left[c_{22}^{*s}h_s z_s + c_{22}^{*a}h_a z_a + (e_{32}^{*s}z_s - G_p e_{32}^{*a}z_a)\frac{e_{32}^{*s}}{\epsilon_{33}^{*s}}h_s\right],$$

$$K_{yy4} = -\left[\frac{1}{12}c_{22}^{c}h_c^3 + c_{22}^{*s}\left(z_s^2 h_s + \frac{1}{12}h_s^3\right) + c_{22}^{*a}\left(z_a^2 h_a + \frac{1}{12}h_a^3\right) + (e_{32}^{*s}z_s - G_p e_{32}^{*a}z_a)\frac{e_{32}^{*s}}{\epsilon_{33}^{*s}}h_s z_s + \left(\frac{h_s^3}{12}\frac{\left(e_{32}^{*s}\right)^2}{\epsilon_{33}^{*s}} + \frac{h_a^3}{12}\frac{\left(e_{32}^{*a}\right)^2}{\epsilon_{33}^{*a}}\right)\right],$$

$$K_{yy5} = -\frac{e_{32}^{*a} e_{31}^{*s}}{\epsilon_{33}^{*s}} G_d h_s z_a,$$

$$K_{yy6} = -\frac{e_{32}^{*a} e_{31}^{*s}}{\epsilon_{33}^{*s}} G_d h_s z_s z_a,$$

$$K_{yy7} = -\frac{e_{32}^{*a} e_{32}^{*s}}{\epsilon_{33}^{*s}} G_d h_s z_a,$$

$$K_{yy8} = -\frac{e_{32}^{*a} e_{32}^{*s}}{\epsilon_{33}^{*s}} G_d h_s z_s z_a,$$

$$K_{xy1} = \frac{1}{2}[2c_{66}^{*s} z_s h_s + 2c_{66}^{*a} z_a h_a],$$

$$K_{xy2} = -\left[\frac{1}{6} c_{66}^{c} h_c^3 + 2c_{66}^{*s}\left(z_s^2 h_s + \frac{1}{12} h_s^3\right) + 2c_{66}^{*a}\left(z_a^2 h_a + \frac{1}{12} h_a^3\right)\right]$$

$$c_1 = \frac{\left(j^4 K_{yy4} L_x^4 + i^2 j^2 \left(K_{xx4} + 2K_{xy2} + K_{yy2}\right) L_x^2 L_y^2 + i^4 K_{xx2} L_y^4\right)\pi^4}{4 L_x^3 L_y^3}, \tag{A.10}$$

$$c_2 = \frac{1}{L_x^3 L_y^3 m\left(-4j^2 + m^2\right) n\left(-4i^2 + n^2\right)} 16 i^2 j^2 \left(L_x^2 m^2 \left(i^2 L_y^2 \left(J_{xx4} + J_{yy2} - K_{xx3} + K_{xy1}\right) + L_x^2 \left(j^2 \left(2J_{yy4} + 3K_{yy3}\right) - K_{yy3} m^2\right)\right)\right.$$
$$\left. + L_y^2 \left(i^2 (2J_{xx2} + 3K_{xx1}) L_y^2 + L_x^2 \left(j^2 \left(J_{xx4} + J_{yy2} + K_{xy1} - K_{yy1}\right) + \left(J_{xy2} - K_{xy1}\right) m^2\right)\right) n^2 - K_{xx1} L_y^4 n^4\right)\pi^2,$$

$$c_3 = 1/c_3^* \left(4\pi^2 ijklmn \left((-1)^{i+k+n} - 1\right)\left((-1)^{j+l+m} - 1\right)\left(j^2 L_x^2 \left(L_y^2 \left(i^2 \left(J_{xy2} + K_{xx3} + K_{xy1} + K_{yy1}\right) - \left(J_{xy2}\right.\right.\right.\right.\right.$$
$$\left.\left.\left.\left.\left. + K_{yy1}\right)\left(k^2 + n^2\right)\right) + K_{yy3} L_x^2 \left(l^2 + m^2\right)\right) + L_y^2 n^2 \left(L_y^2 \left(i^2 K_{xx1} + 2k^2 (J_{xx2} + K_{xx1})\right) + L_x^2 \left(l^2 \left(J_{xx4} + J_{xy2}\right.\right.\right.\right.\right.$$
$$\left.\left.\left.\left.\left. + J_{yy2} + K_{xy1}\right) + m^2 \left(J_{xy2} - K_{xy1}\right)\right)\right) - i^2 J_{xy2} l^2 L_x^2 L_y^2 - i^2 J_{xy2} L_x^2 L_y^2 m^2 + i^2 k^2 K_{xx1} L_y^4 - i^2 K_{xx3} l^2 L_x^2 L_y^2$$
$$- i^2 K_{xx3} L_x^2 L_y^2 m^2 + J_{xx4} k^2 L_x^2 L_y^2 m^2 + J_{xy2} k^2 l^2 L_x^2 L_y^2 + J_{xy2} k^2 L_x^2 L_y^2 m^2 + J_{yy2} k^2 L_x^2 L_y^2 m^2 + 2J_{yy4} l^2 L_x^4 m^2$$
$$\left. - k^4 K_{xx1} L_y^4 - k^2 K_{xy1} l^2 L_x^2 L_y^2 + k^2 K_{xy1} L_x^2 L_y^2 m^2 - K_{xx1} L_y^4 n^4 - K_{yy3} L_x^4 \left(l^2 - m^2\right)^2\right)\right),$$

$$c_3^* = \left(L_x^3 L_y^3 (i - k - n)(i + k - n)(i - k + n)(i + k + n)(j - l - m)(j + l - m)(j - l + m)(j + l + m)\right),$$

$$c_4 = \left(\frac{\pi^2}{36 ij L_x^3 L_y^3}\right)\left(24\left(j^4 J_{yy4} L_x^4 + i^2 j^2 \left(J_{xx4} + J_{xy2} + J_{yy2} - K_{xx3}\right) L_x^2 L_y^2 + i^4 (J_{xx2} + K_{xx1}) L_y^4\right) - 8\left(j^4 \left(J_{yy4}\right.\right.\right.$$
$$\left.\left.\left. + 4K_{yy3}\right) L_x^4 + i^2 j^2 \left(J_{xx4} - J_{xy2} + J_{yy2} + K_{xx3} + 2K_{xy1} - 2K_{yy1}\right) L_x^2 L_y^2 + i^4 (J_{xx2} + K_{xx1}) L_y^4\right)(2\cos(j\pi) + 1)$$
$$+ \cos(3i\pi)\left(3\left(j^4 J_{yy4} L_x^4 + i^2 j^2 \left(J_{xx4} - 2J_{xy2} + J_{yy2} - 4K_{xx3}\right) L_x^2 L_y^2 + i^4 (J_{xx2} + 4K_{xx1}) L_y^4\right) - \left(j^4 \left(J_{yy4}\right.\right.\right.$$
$$\left.\left.\left. + 4K_{yy3}\right) L_x^4 + i^2 j^2 \left(J_{xx4} + 2J_{xy2} + J_{yy2} + 4\left(K_{xx3} + 2K_{xy1} + K_{yy1}\right)\right) L_x^2 L_y^2 + i^4 (J_{xx2} + 4K_{xx1}) L_y^4\right)(2\cos(j\pi)$$
$$\left. + 1)) + 3\cos(i\pi)\left(-9j^4 J_{yy4} L_x^4 - 3i^2 j^2 \left(3J_{xx4} + 2J_{xy2} + 3J_{yy2} - 4K_{xx3}\right) L_x^2 L_y^2 - 3i^4 (3J_{xx2} + 4K_{xx1}) L_y^4\right.$$
$$+ \left(3j^4 \left(J_{yy4} + 4K_{yy3}\right) L_x^4 + i^2 j^2 \left(3J_{xx4} - 2J_{xy2} + 3J_{yy2} + 4K_{xx3} + 8K_{xy1} - 4K_{yy1}\right) L_x^2 L_y^2 + i^4 (3J_{xx2}\right.$$
$$\left.\left. + 4K_{xx1}) L_y^4\right)\ (2\cos(j\pi) + 1))),$$

$$c_5 = \left(1/\left(ijL_x^3 L_y^3 \left(j^2 - 4m^2\right)\left(i^2 - 4n^2\right)\right)\right) 8 m^2 n^2 \left(i^2 L_y^2 \left(L_x^2 \left(j^2 \left(J_{xy2} + K_{xx3} + K_{xy1} + K_{yy1}\right) - 2\left(J_{xy2}\right.\right.\right.\right.$$
$$\left.\left.\left.\left. + K_{xx3}) m^2\right) + 2K_{xx1} L_y^2 n^2\right) + 2\left(L_x^4 m^2 \left(j^2 K_{yy3} + J_{yy4} m^2\right) + L_x^2 L_y^2 \left(\left(-j^2\right)\left(J_{xy2} + K_{yy1}\right) + \left(J_{xx4} + 2J_{xy2}\right.\right.\right.\right.$$
$$\left.\left.\left.\left. + J_{yy2}\right) m^2\right)\ n^2 + J_{xx2} L_y^4 n^4\right)\right)\pi^2,$$

$$c_6 = -\left(\frac{\left(3j^4 J_{yy3} L_x^4 + i^2 j^2 \left(3J_{xx3} - 2J_{xy1} + 3J_{yy1}\right) L_x^2 L_y^2 + 3i^4 J_{xx1} L_y^4\right)\pi^4}{64 L_x^3 L_y^3}\right),$$

$$c_7 = -\left(\frac{3\left(j^4 J_{yy7} L_x^4 + i^2 j^2 \left(J_{xx7} + J_{yy5}\right) L_x^2 L_y^2 + i^4 J_{xx5} L_y^4\right)\pi^4}{64 L_x^3 L_y^3}\right),$$

$$c_8 = -\left(\frac{\left(i^2L_y^2\left(J_{xx3}L_x^2m^2 + J_{xx1}L_y^2n^2\right) + j^2\left(J_{yy3}L_x^4m^2 + J_{yy1}L_x^2L_y^2n^2\right)\right)\pi^4}{16L_x^3L_y^3}\right),$$

$$c_9 = \frac{\left(j^4K_{yy8}L_x^4 + i^2j^2\left(K_{xx8} + K_{yy6}\right)L_x^2L_y^2 + i^4K_{xx6}L_y^4\right)\pi^4}{4L_x^3L_y^3},$$

$$\begin{aligned}c_{10} = {} & \left(\frac{\pi^2}{36ijL_x^3L_y^3}\right)\left(24\left(j^4J_{yy8}L_x^4 + i^2j^2\left(J_{xx8} + J_{yy6} - K_{xx7}\right)L_x^2L_y^2 + i^4(J_{xx6} + K_{xx5})L_y^4\right) - 8\left(j^4\left(J_{yy8}\right.\right.\right.\\ & \left.\left.\left.+4K_{yy7}\right)L_x^4 + i^2j^2\left(J_{xx8} + J_{yy6} + K_{xx7} - 2K_{yy5}\right)L_x^2L_y^2 + i^4\left(J_{xx6} + K_{xx5}\right)L_y^4\right)(2\cos(j\pi) + 1)\right.\\ & \left.+\cos(3i\pi)\left(3\left(j^4J_{yy8}L_x^4 + i^2j^2\left(J_{xx8} + J_{yy6} - 4K_{xx7}\right)L_x^2L_y^2 + i^4\left(J_{xx6} + 4K_{xx5}\right)L_y^4\right) - \left(j^4\left(J_{yy8} + 4K_{yy7}\right)L_x^4\right.\right.\right.\\ & \left.\left.\left.+i^2j^2\left(J_{xx8} + J_{yy6} + 4\left(K_{xx7} + K_{yy5}\right)\right)L_x^2L_y^2 + i^4\left(J_{xx6} + 4K_{xx5}\right)L_y^4\right)(2\cos(j\pi) + 1)\right) + 3\cos(i\pi)\left(-9j^4J_{yy8}L_x^4\right.\right.\\ & \left.\left.-3i^2j^2\left(3\left(J_{xx8} + J_{yy6}\right) - 4K_{xx7}\right)L_x^2L_y^2 - 3i^4(3J_{xx6} + 4K_{xx5})L_y^4 + \left(3j^4\left(J_{yy8} + 4K_{yy7}\right)L_x^4 + i^2j^2(3J_{xx8}\right.\right.\right.\\ & \left.\left.\left.+3J_{yy6} + 4K_{xx7} - 4K_{yy5}\right)L_x^2L_y^2 + i^4(3J_{xx6} + 4K_{xx5})L_y^4\right)(2\cos(j\pi) + 1))),\end{aligned}$$

$$\begin{aligned}c_{11} = {} & \frac{1}{L_x^3L_y^3m\left(-4j^2 + m^2\right)n\left(-4i^2 + n^2\right)}\left(8i^2j^2\left(L_x^2m^2\left(i^2\left(2J_{yy6} - K_{xx7}\right)L_y^2 + L_x^2\left(j^2\left(2J_{yy8} + 3K_{yy7}\right)\right.\right.\right.\right.\\ & \left.\left.\left.\left.-K_{yy7}m^2\right)\right) + L_y^2\left(j^2\left(2J_{xx8} - K_{yy5}\right)L_x^2 + i^2(2J_{xx6} + 3K_{xx5})L_y^2\right)n^2 - K_{xx5}L_y^4n^4\right)\pi^2\right),\end{aligned}$$

$$\begin{aligned}c_{12} = {} & \frac{1}{L_x^3L_y^3m\left(-4j^2 + m^2\right)n\left(-4i^2 + n^2\right)}\left(8i^2j^2\left(L_x^2m^2\left(i^2\left(2J_{xx8} - K_{xx7}\right)L_y^2 + L_x^2\left(j^2\left(2J_{yy8} + 3K_{yy7}\right)\right.\right.\right.\right.\\ & \left.\left.\left.\left.-K_{yy7}m^2\right)\right) + L_y^2\left(j^2\left(2J_{yy6} - K_{yy5}\right)L_x^2 + i^2(2J_{xx6} + 3K_{xx5})L_y^2\right)n^2 - K_{xx5}L_y^4n^4\right)\pi^2\right),\end{aligned}$$

$$c_{13} = -\left(\frac{\left(i^2L_y^2\left(J_{xx7}L_x^2m^2 + J_{xx5}L_y^2n^2\right) + j^2\left(J_{yy7}L_x^4m^2 + J_{yy5}L_x^2L_y^2n^2\right)\right)\pi^4}{16L_x^3L_y^3}\right),$$

$$\begin{aligned}c_{14} = {} & \frac{1}{c_3^*}\left(2ijklmn\left(\left(-i^2\right)K_{xx7}l^2L_x^2L_y^2 + i^2k^2K_{xx5}L_y^4 - k^4K_{xx5}L_y^4 + 2J_{yy8}l^2L_x^4m^2 + 2J_{xx8}k^2L_x^2L_y^2m^2\right.\right.\\ & -i^2K_{xx7}L_x^2L_y^2m^2 - K_{yy7}L_x^4\left(l^2 - m^2\right)^2 + L_y^2\left(2J_{yy6}l^2L_x^2 + \left(i^2K_{xx5} + 2k^2\left(J_{xx6} + K_{xx5}\right)\right)L_y^2\right)n^2\\ & \left.-K_{xx5}L_y^4n^4 + j^2L_x^2\left(K_{yy7}L_x^2\left(l^2 + m^2\right) + L_y^2\left(i^2\left(K_{xx7} + K_{yy5}\right) - K_{yy5}\left(k^2 + n^2\right)\right)\right)\right)\pi^2(-1\\ & \left.+(-1)^{j+l+m}\right)\left(-1 + (-1)^{i+k+n}\right)\Big),\end{aligned}$$

$$\begin{aligned}c_{15} = {} & \frac{1}{ijL_x^3L_y^3\left(j^2 - 4m^2\right)\left(i^2 - 4n^2\right)}\left(8m^2n^2\left(i^2L_y^2\left(L_x^2\left(j^2\left(K_{xx7} + K_{yy5}\right) - 2K_{xx7}m^2\right) + 2K_{xx5}L_y^2n^2\right)\right.\right.\\ & \left.\left.+2\left(L_x^4m^2\left(j^2K_{yy7} + J_{yy8}m^2\right) + L_x^2L_y^2\left(\left(-j^2\right)K_{yy5} + \left(J_{xx8} + J_{yy6}\right)m^2\right)n^2 + J_{xx6}L_y^4n^4\right)\right)\pi^2\right),\end{aligned}$$

$$c_{16} = -\frac{I_0L_xL_y}{4} - \frac{I_2\left(j^2L_x^2 + i^2L_y^2\right)\pi^2}{4L_xL_y},$$

$$c_{17} = \frac{4I_1iL_y\left(-1 + \cos(i\pi)^3\right)(2 + \cos(j\pi))}{9jL_x} - \frac{4I_1jL_x(2 + \cos(i\pi))(4 + 2\cos(j\pi))}{9iL_y},$$

$$c_{18} = \frac{-8I_1i^2j^2\left(L_x^2m^2 + L_y^2n^2\right)}{L_xL_ym\left(-4j^2 + m^2\right)n\left(-4i^2 + n^2\right)},$$

$$c_{19} = \frac{8I_1m^2n^2\left(L_x^2\left(j^2 - 2m^2\right) + L_y^2\left(i^2 - 2n^2\right)\right)}{ijL_xL_y\left(j^2 - 4m^2\right)\left(i^2 - 4n^2\right)},$$

$$c_{20} = \frac{2I_1ijklmn\left(j^2L_x^2 - L_x^2\left(l^2 + m^2\right) + L_y^2\left(i^2 - k^2 - n^2\right)\right)}{L_xL_y(j - l - m)(j + l - m)(j - l + m)(j + l + m)}\frac{\left(-1 + (-1)^{j+l+m}\right)\left(-1 + (-1)^{i+k+n}\right)}{(i - k - n)(i + k - n)(i - k + n)}.$$

Appendix B

Following the standard approach in harmonic balance method explained in Section 3.2 and using the transformation $A=re^{i\theta}$, Eq. (B.1) can be obtained that provides the relation between the nonlinear transverse vibration with respect to frequency of the excitation [18,19,28,29]

$$r^6|K_{NL}|^2+r^4\left[2\left(K^RK_{NL}^R+K^IK_{NL}^I\right)-2\omega^2MK_{NL}^R\right]+r^2\left(\omega^4M^2+|K|^2-2\omega^2MK^R\right)-Q^2=0, \tag{B.1}$$

where,

$$M=-\frac{1}{4}I_0L_xL_y-\frac{I_2\left(L_x^2+L_y^2\right)\pi^2}{4L_xL_y},$$

$$K(\omega)=K^R+iK^I(\omega)=|K|e^{i\alpha},$$

$$K_{NL}=K_{NL}^R+iK_{NL}^I(\omega)=|K_{NL}|e^{i\beta},$$

$$K^R=\frac{\left(K_{yy4}L_x^4+\left(K_{xx4}+2K_{xy2}+K_{yy2}\right)L_x^2L_y^2+K_{xx2}L_y^4\right)\pi^4}{4L_x^3L_y^3},$$

$$K^I(\omega)=\frac{\left(K_{yy8}L_x^4+\left(K_{xx8}+K_{yy6}\right)L_x^2L_y^2+K_{xx6}L_y^4\right)\pi^4\omega}{4L_x^3L_y^3},$$

$$K_{NL}^R=-\frac{3\left(3J_{yy3}L_x^4+\left(3J_{xx3}-2J_{xy1}+3J_{yy1}\right)L_x^2L_y^2+3J_{xx1}L_y^4\right)\pi^4}{64L_x^3L_y^3},$$

$$K_{NL}^I(\omega)=-\frac{3\left(J_{yy7}L_x^4+\left(J_{xx7}+J_{yy5}\right)L_x^2L_y^2+J_{xx5}L_y^4\right)\pi^4\omega}{64L_x^3L_y^3},$$

$$Q=-\frac{4BL_xL_y}{\pi^2}. \tag{B.2}$$

Eq. (B.1) should be solved numerically. The solution presented above is obtained for the first harmonic of the piezolaminated plate and the higher order modes can be obtained by changing m, n accordingly.

Remark B1. The Notebook file (.nb) compatible with Wolfram Mathematica that includes the sensitivity analysis of the frequency domain response for single mode vibration analysis is available for the interested reader. This file provides the closed form solution that evaluates the transverse normalized vibration (w_{0f}/h) amplitude with respect to frequency of the distributed harmonic external excitation (see Section 3.2). It should be pointed out that following the same trend for transient response of the smart structure, the results in frequency domain are presented only for simply supported boundary conditions. However, as long as the shape functions are available for a problem-specific boundary condition the combination of the Galerkin method and harmonic balance technique can be employed.

References

[1] Wagg D, Neild S. Nonlinear vibration with control: for flexible and adaptive structures. New York: Springer Science; 2010.
[2] Lacarbonara W, Chin C, Soper RR. Open-loop nonlinear vibration control of shallow arches via perturbation approach. Trans ASME J Appl Mech 2002;69(3):325–34.
[3] Mahmoodi SN, Jalili N, Daqaq MF. Modeling, nonlinear dynamics, and identification of a piezoelectrically actuated microcantilever sensor. IEEE/ASME Trans Mechatron 2008;13(1):58–65.
[4] Jun L, Xiaobin L, Hongxing H. Active nonlinear saturation-based control for suppressing the free vibration of a self-excited plant. Commun Nonlinear Sci Numer Simul 2010;15(4):1071–9.
[5] Oveisi A, Shakeri R. Robust reliable control in vibration suppression of sandwich circular plates. Eng Struct 2016;116:1–11.
[6] Ghandchi Tehrani M, Wilmshurst L, Elliott SJ. Receptance method for active vibration control of a nonlinear system. J Sound Vib 2013;332(19):4440–9.
[7] Oveisi A, Nestorović T. Robust observer-based adaptive fuzzy sliding mode controller. Mech Syst Signal Pr 2016;76:58–71.
[8] Soize C. Random matrix theory for modeling uncertainties in computational mechanics. Comput Method Appl M 2005;194(12-16):1333–66.
[9] Adhikari S, Friswell MI, Lonkar K, Sarkar A. Experimental case studies for uncertainty quantification in structural dynamics. Probabilist Eng Mech 2009;24:473–92.
[10] Oveisi A, Nestorović T. Robust nonfragile observer-based H_2/H_∞ controller. J Vib Control 2016:1–17.
[11] Kozien MS, Kołtowski B. Comparison of active and passive damping of plate vibration by piezoelectric actuators — FEM simulation. Acta Phys Pol A 2011;119:1005–8.
[12] Casado CM, Díaz IM, de Sebastián J, Poncela AV, Lorenzana A. Implementation of passive and active vibration control on an in-service footbridge. Struct Control Hlth 2013;20(1):70–87.
[13] Hasheminejad SM, Oveisi A. Active vibration control of an arbitrary thick smart cylindrical panel with optimally placed piezoelectric sensor/actuator pairs. Int J Mech Mater Des 2015. doi:10.1007/s10999-015-9293-2.
[14] Stojanović V. Geometrically nonlinear vibrations of beams supported by a nonlinear elastic foundation with variable discontinuity. Commun Nonlinear Sci Numer Simul 2015;28:66–80.

[15] Borowiec M, Litak G, Friswell MI, Adhikari S. Energy harvesting in a nonlinear cantilever piezoelastic beam system excited by random vertical vibrations international. Int J Struct Stab Dyn 2014;14(8).
[16] Jayakumar K, Yadav D, Nageswara Rao B. Nonlinear free vibration analysis of simply supported piezo-laminated plates with random actuation electric potential difference and material properties. Commun Nonlinear Sci Numer Simul 2009;14(4):1646–63.
[17] Moita JMS, Soares CMM, Soares CAM. Geometrically non-linear analysis of composite structures with integrated piezoelectric sensors and actuators. Compos Struct 2002;57(1-4):253–61.
[18] Gao JX, Shen YP. Active control of geometrically nonlinear transient vibration of composite plates with piezoelectric actuators. J Sound Vib 2003;264(4):911–28.
[19] Belouettar S, Azrar L, Daya EM, Laptev V, Potier-Ferryc M. Active control of nonlinear vibration of sandwich piezoelectric beams: a simplified approach. Comput Struct 2008;86(3-5):386–97.
[20] Ray MC, Shivakumar J. Active constrained layer damping of geometrically nonlinear transient vibrations of composite plates using piezoelectric fiber-reinforced composite. Thin Wall Struct 2009;47(2):178–89.
[21] Warminski J, Bochenski M, Jarzyna W, Filipek P, Augustyniak M. Active suppression of nonlinear composite beam vibrations by selected control algorithms. Commun Nonlinear Sci Numer Simul 2011;16(5):2237–48.
[22] Oveisi A, Gudarzi M. Nonlinear robust vibration control of a plate integrated with piezoelectric actuator. Int J Math Mod Meth App Sci 2013;7(6):638–46.
[23] Oveisi A, Gudarzi M. Adaptive sliding mode vibration control of a nonlinear smart beam: a comparison with self-tuning Ziegler–Nichols PID controller. J Low Freq Noise V A 2013;31(1-2):41–62.
[24] Damanpack AR, Bodaghi M, Aghdam MM, Shakeri M. Active control of geometrically non-linear transient response of sandwich beams with a flexible core using piezoelectric patches. Compos Struct 2013;100:517–31.
[25] Chee CYK, Tong L, Steven GP. A review on the modelling of piezoelectric sensors and actuators incorporated in intelligent structures. J Intel Mat Syst Str 1998;9(1):3–19.
[26] Yang S, Huang W. Piezoelectric constitutive equations for a plate shape sensor/actuator. AIAA J 1997;35(12):1894–5.
[27] Mota Soares CM, Mota Soares CA, Franco Correi VM. Optimal design of piezolaminated structures. Compos Struct 1999;47:625–34.
[28] Oveisi A, Nestorović T, Nguyen N. Semi-analytical modeling and vibration control of a geometrically nonlinear plate. Int J Struct Stab Dyn 2017;17(4):1771003-1–1771003-12. doi:10.1142/S0219455417710031.
[29] Rechdaoui MS, Azrar L. Stability and nonlinear dynamic analyses of beam with piezoelectric actuator and sensor based on higher-order multiple scales methods. Int J Struct Stab Dyn 2013;13(8).